2011 50th IEEE Conference on Decision and Control and
European Control Conference (CDC-ECC)
Orlando, FL, USA, December 12-15, 2011

Cascade and multibatch subspace system identification for multivariate vacuum-plasma response characterisation

Erik Olofsson[1], Cristian R. Rojas[2], Håkan Hjalmarsson[2], Per Brunsell[1] and James R. Drake[1]

Abstract— **A particular cascade structure system identification problem is formulated for the purpose of characterising the vacuum-plasma response for a magnetic confinement fusion experiment. A predictor-form closed-loop subspace system identification approach is advocated due to (i) plant instability (ii) sizes of input-output vectors and (iii) inherent multivariate eigenmodes of the physical system. Since experiment data come in relatively short batches, specialised means for data merging for subspace identification are developed. A batchwise delete-group jackknife procedure is utilised to estimate the standard error of the estimate of the dominant unstable empirical plasma response eigenvalue.**

I. INTRODUCTION

The development of magnetic confinement thermonuclear fusion (MCF) power plants involves many scientific and technologial challenges [1], [2], [3]. MCF aims to confine an ionised hydrogen isotope gas mainly using strong (several Teslas) magnetic fields, of which the bulk is generated by external superconducting coils and an internal electrical current. The ionised gas-like state of matter is known as the plasma state. Thermonuclear fusion of the two hydrogen isotopes deuterium and tritium (D-T) appears most easy to attain. The cross-section for D-T fusion essentially requires a plasma thermal energy of $\sim 10^8$ Kelvins for reactor-grade amplification of input heating power. This temperature is significantly higher than the innards of the sun (but the required matter density is much lower). A fusion reactor is dimensioned at a length scale of several meters. It may not come as a surprise, then, that an assortment of instabilities tend to develop in a machine designed to sustain the implied temperature gradients in a steady-state. The multibillion-euro international flagship experiment reactor ITER [4], just starting to be built in France, is designed to provide substantial answers to the scientific and engineering feasibility issues of MCF.

Some specific issues for identification and control of magnetohydrodynamic (MHD) stability of toroidal MCF machines are considered in this work. MHD is the main continuum fluid theory for modeling (global) plasma stability [5], [6]. MHD stability feedback control is expected to be a key technology for future reactors [7]. A particular MHD instability is the resistive wall mode (RWM) thought to set limitations on the efficiency of power generation in advanced MCF reactors [8]. Other MHD-related research suggests that empirical separation of vacuum and plasma response contributions to the full magnetic field could be crucial for the ability to mitigate certain edge-localised MHD instabilitites [9]. The ambition here is to begin development and application of subspace system identification methods (SIMs) [10], [11] to provide useful techniques for (i) improvement of plasma control and (ii) novel scientific measurements of in situ plasma stability. The latter implies some estimation of uncertainty of the estimates.

SIMs can handle general discrete-time multi-input multi-output (MIMO) linear time-invariant (LTI) state-space systems [11] and quite recently also closed-loop datasets [10], [12]. The computational basis in numerical linear algebra makes SIMs applicable for quite large MIMO plants. Cascade structures and merging of data are recurring themes in SIM applications [13]. These topics are both given particular treatment in the present work.

This paper is organised as follows. Section II outlines the experimental MCF plant and the control circuitry. The identification problem is detailed herein and the approaches to solving it are declared. Section III introduces the notations of SIMs and proposes a batchified modification of an established SIM from the literature. Jackknife uncertainty estimation from computational statistics are then adapted for the batchwise partitioning of data which is natural here. Section IV then employs the above methods to datasets from the MCF experiment. Results are presented for the top plasma response eigenvalue, including standard errors, using various cascade-based SIM recipes. Conclusions are given in the final section V.

II. CASCADE APPROACHES AND VACUUM-PLASMA SEPARATION

The signal schematic for the feedback control system for nonaxisymmetric stabilisation of the MCF plant EXTRAP T2R (T2R) is shown in Figure 1. T2R is briefly introduced in subsection II-A where the signals in Figure 1 will be given physical meaning. In subsections II-B and II-C the structural aspects of the interconnections are considered.

The first consideration of cascade structure, subsection II-B, is an attempt to avoid (or assess impact of) the potential errors-in-variables problem [14] associated with the direct identification, from $\tilde{\mathbf{u}}$ to $\mathbf{y}$, of the process of interest G (T2R), which is embedded in a cascade to which $\mathbf{d}$ is the noise free input. The second cascade structure, detailed in subsection II-C, is implicit (not due to data acquisition hardware or software signal routing) and relates to physical modeling of the plant.

[1]School of Electrical Engineering (EES), Royal Institute of Technology (KTH) [2]ACCESS Linnaeus Center KTH/EES, Stockholm, Sweden
Corresponding author email: erik.olofsson@ee.kth.se

978-1-61284-799-3/11/$26.00 ©2011 IEEE

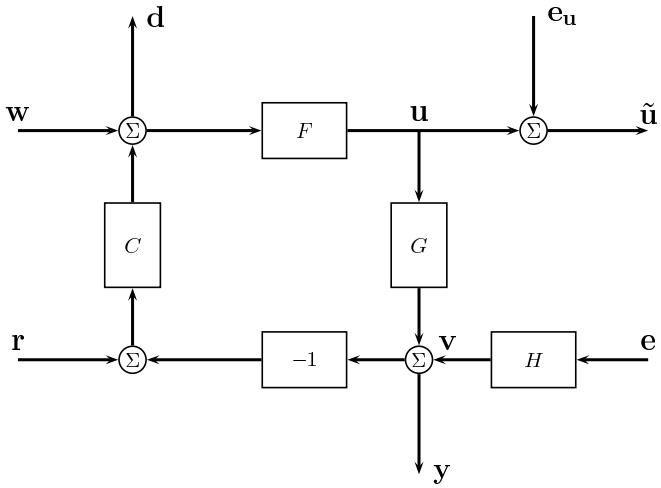

Fig. 1. Signal schematic of closed-loop actuator-process cascade with process input measurement and exogenous dither injection input.

A. The MCF plant: EXTRAP T2R reversed-field pinch

The reversed-field pinch (RFP) [15] is an MCF device in which the toroidal and poloidal magnetic field strengths are of the same order. In the tokamak [3] the toroidal field is an order of magnitude stronger than the poloidal field. The tokamak is currently more progressed in terms of fusion reactor prospects, but RFPs and tokamaks share many MHD stability phenomena, so knowledge transfer is often bidirectional between the devices. EXTRAP T2R (T2R) [16] is an RFP device with particular focus on feedback control of MHD modes [17], [18].

The T2R signals and system blocks of Figure 1 are as follows. $\mathbf{y} \in \mathbb{R}^{64\times 1}$ is the time-integrated voltages from an array of magnetic flux loops wired in saddle-fashion outside the conducting resistive shell of the toroidal plasma chamber. $\tilde{\mathbf{u}} \in \mathbb{R}^{64\times 1}$ is a vector of measured currents in similarly saddle-looped conductors which are actively driven (actuators). $\mathbf{d} \in \mathbb{R}^{64\times 1}$ is the input to the digital-to-analog converter that feeds the power amplifier racks F. G is the T2R plant (the external plasma response). The digital nominal PID controller is denoted C and has the capability to stabilise T2R. $\mathbf{r} \in \mathbb{R}^{64\times 1}$ is the reference for the controller which is zeroed throughout this work, and $\mathbf{w} \in \mathbb{R}^{64\times 1}$ is the dither injection which is generated as described in [18]. The sample-interval is $\tau_s = 0.1\,\mathrm{ms}$.

B. Actuator identification for cascade input filtering

It is well known that errors on the inputs lead to bias in system identification. The presence of $\mathbf{e_u}$ in Figure 1 might therefore be an issue. A direct method to clean-up $\tilde{\mathbf{u}}$ is to first estimate F to form the predictor filter, denoted $\hat{F}$, as detailed in subsection III-A. Then filter out the vector signal

$$\hat{\mathbf{u}}_{\hat{F}} = \hat{F}\begin{pmatrix}\mathbf{d}\\ \tilde{\mathbf{u}}\end{pmatrix} \tag{1}$$

and replace $\tilde{\mathbf{u}}$ with $\hat{\mathbf{u}}_{\hat{F}}$ for subsequent direct identification of the process G.

In the case of measurement noise only (expected case) and an F of modest complexity (also expected) this may help to improve the estimate of G. But if $\mathbf{e_u}$ is insignificant already, this may instead worsen the accuracy of the estimate of G by introducing new errors due to inexactness of $\hat{F}$ and its initial conditions.

C. Cascade structure for plasma response isolation

Figure 2 shows two processes that both take the position of G in Figure 1. G_0 is the magnetic diffusion dynamics (entirely stable) that the dry system (no plasma in the toroidal chamber) exhibits. Therefore G_0 includes the effect of the possibly nontrivial external structures carrying passive eddy-currents. $G_1 = (I + \Gamma)G_0$ is the wet system dynamics (plasma in the toroidal chamber). G_1 is known to be unstable and also sports significant stochastic (e.g. other MHD activity) behaviour alluded by H in Figure 1. When G_0 takes the place of G in schematic 1 H can be set to I and $\mathbf{e}$ can be thought of as very small.

A recurring idea in MHD modeling of plasma stability is to let the total magnetic field be a superposition of terms from (i) sources external to the plasma and (ii) sources internal to the plasma [19], [8], [20]. The approach here is to confine the plasma response to the system Γ as depicted in the bottom of Figure 2. This essentially means that $I + \Gamma$ is the linear permeability system as detailed in [20]. It is then expected that the plasma eigenvalues are solely inside Γ.

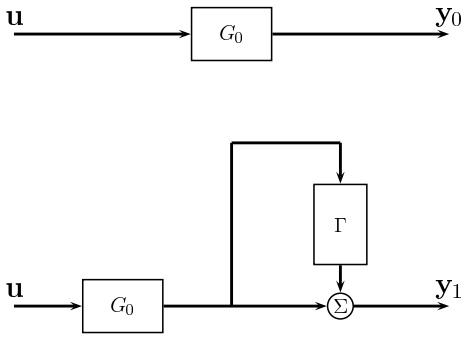

Fig. 2. G_0 vacuum field diffusion and $G_1 = (I+\Gamma)G_0$ plasma response cascade model. Nondimensional plasma permeability is $I + \Gamma$. Plasma eigenvalues are supposed to reside in system Γ.

Assume now that an estimate of the vacuum system $\hat{G}_0$ is given. Provided a dataset $\{\mathbf{u}_1, \mathbf{y}_1\}$ acquired from plasma experiments it is possible to simulate $\hat{\mathbf{y}}_{0|1} = \hat{G}_0\mathbf{u}_1$ and then identify either of

1) the system $I + \Gamma$ with input $\hat{\mathbf{y}}_{0|1}$ and output $\mathbf{y}_1$.
2) the system Γ with input $\hat{\mathbf{y}}_{0|1}$ and output $\delta\mathbf{y} = \mathbf{y}_1 - \hat{\mathbf{y}}_{0|1}$.

This will be done in the data analysis of section IV below using the multibatch signal processing introduced in the next section III.

III. SUBSPACE SYSTEM IDENTIFICATION WITH BATCH MANAGEMENT

A. Standard representations of discrete-time LTI systems

The usual innovation and predictor forms of multi-input multi-output (MIMO) linear time-invariant discrete-time systems are central for the formulation of SIMs [10]. The innovation form of the LTI system (A, B, C, D, K) is given by

$$\begin{aligned} \hat{\mathbf{x}}(k+1) &= A\hat{\mathbf{x}}(k) + B\mathbf{u}(k) + K\mathbf{e}(k) && \text{(2a)} \\ \mathbf{y}(k) &= C\hat{\mathbf{x}}(k) + D\mathbf{u}(k) + \mathbf{e}(k) && \text{(2b)} \end{aligned}$$

The related predictor form is

$$\begin{aligned} \hat{\mathbf{x}}(k+1) &= A_K\hat{\mathbf{x}}(k) + B_K\mathbf{z}(k) && \text{(3a)} \\ \mathbf{y}(k) &= C\hat{\mathbf{x}}(k) + D\mathbf{u}(k) + \mathbf{e}(k) && \text{(3b)} \end{aligned}$$

with

$$\begin{aligned} A_K &= A - KC && \text{(4a)} \\ B_K &= \begin{pmatrix} B - KD & K \end{pmatrix} && \text{(4b)} \end{aligned}$$

and the stacked signal

$$\mathbf{z}(k) = \begin{pmatrix} \mathbf{u}(k) \\ \mathbf{y}(k) \end{pmatrix} \tag{5}$$

The hat symbol in equations (2) and (3) imply state estimate status. The innovation sequence is $\{\mathbf{e}(k)\}$. The predictor *filter* form (3) is obtained by (i) removal of the innovation from output equation (3b) and (ii) substitution of $\hat{\mathbf{y}}$ for $\mathbf{y}$ in (3b).

A generic MIMO plant (stable or unstable) where $\mathbf{u}(k) \in \mathbb{R}^{n_u \times 1}$ and $\mathbf{y}(k) \in \mathbb{R}^{n_y \times 1}$ is considered in the following subsections.

B. Merging of multiple batches in subspace identification

Particular modifications of the standard SIMs are required to properly handle multiple datasets. Let $\mathcal{D}_b = \left\{\mathbf{y}^{(b)}(k), \mathbf{u}^{(b)}(k)\right\}_{k=1}^{N_b}$ be a single set of experimental input and output vector data. The experiment is indexed by b and the length of the recording is N_b. $\mathcal{D}_b$ will be referred to as a *batch* in the following. Denote the complete available set of batches be $\mathcal{D}_\mathcal{B} = \{\mathcal{D}_b\}_{b=1}^{n_b}$ where n_b is the number of batches. The complete number of time-samples is $\sum_{b=1}^{n_b} N_b$. The aim of the next subsection is to incorporate this data in an established SIM in a sensible way. The SIM of choice is the SSARX method due to Jansson [12] which utilises a vector autoregressive exogenous (VARX) preestimation step to be able to cope with closed-loop acquired datasets. The VARX preestimation may also act as an order selection for the future and past horizons associated to the SIM.

C. Multibatch VARX preestimation with cross-validation

Define the past lag vector

$$\mathbf{z}_p(k) = \begin{pmatrix} \mathbf{z}(k-1) \\ \vdots \\ \mathbf{z}(k-p) \end{pmatrix} \tag{6}$$

where $\mathbf{z}(k)$ is the joint signal (5). Let $\mathbf{z}_p^{(b)}(k)$ denote the past lag vector (6) made from batch data $\mathcal{D}_b$. Introduce

$$\begin{aligned} Y_q^{(b)} &= \begin{pmatrix} \mathbf{y}^{(b)}(q+1) & \dots & \mathbf{y}^{(b)}(N_b) \end{pmatrix} && \text{(7a)} \\ Z_q^{(b)} &= \begin{pmatrix} \mathbf{z}_q^{(b)}(q+1) & \dots & \mathbf{z}_q^{(b)}(N_b) \\ \mathbf{u}^{(b)}(q+1) & \dots & \mathbf{u}^{(b)}(N_b) \end{pmatrix} && \text{(7b)} \end{aligned}$$

where q is the VARX lag order. Batch data matrices (7) are then merged as follows.

$$\begin{aligned} Y_q &= \begin{pmatrix} Y_q^{(1)} & \dots & Y_q^{(n_b)} \end{pmatrix} && \text{(8a)} \\ Z_q &= \begin{pmatrix} Z_q^{(1)} & \dots & Z_q^{(n_b)} \end{pmatrix} && \text{(8b)} \end{aligned}$$

All batches are thus accounted for in the standard least-squares estimation problem

$$\begin{aligned} \hat{H}_q &= \arg\min_{H_q} \|Y_q - H_q Z_q\|_F^2 \\ &= Y_q Z_q^T \left(Z_q Z_q^T\right)^{-1} && \text{(9)} \end{aligned}$$

where $\|\cdot\|_F$ denotes the Frobenius matrix norm $\|M\|_F = \sqrt{\mathrm{tr}\,(MM^T)}$ and $\mathrm{tr}\,(\cdot)$ matrix trace [10], [21], [22]. The argument lag-q predictor-form Markov coefficient matrix in (9) has the structure

$$H_q = \begin{pmatrix} H(1) & \dots & H(q) & D_q \end{pmatrix} \tag{10}$$

with D_q being the direct feedthrough.

Lag order selection can be suggested by cross-validation as described in the following. Select a column group size r and find the largest integer g such that rg is less than or equal to the number of columns in (8). Let Y_q^1 denote the first r columns of Y_q, Y_q^2 columns $r+1 \dots 2r$ and so on. Employ an analogous notation for submatrices of Z_q. For each lag-order q, repeatedly compute

$$\begin{aligned} \hat{H}_q^j &= \left(Y_q Z_q^T - Y_q^j Z_q^{j\,T}\right)\left(Z_q Z_q^T - Z_q^j Z_q^{j\,T}\right)^{-1} && \text{(11a)} \\ \hat{E}_q^j &= Y_q^j - \hat{H}_q Z_q^j && \text{(11b)} \end{aligned}$$

for $j = 1 \dots g$ to be able to evaluate

$$\rho_{CV}(q,r) = \left(\sum_{j=1}^{g(r)} \mathrm{tr}\left(\hat{E}_q^j \hat{E}_q^{j\,T}\right)\right) / \eta(q,r) \tag{12}$$

where $\eta(q,r) = \sum_{j=1}^{g(r)} \mathrm{tr}\left(Y_q^j Y_q^{j\,T}\right)$. Assume that r is small enough to only weakly influence (12). The simplification $\rho_{CV}(q,r) = \rho_{CV}(q)$ then results in a lag selection heuristic $q^\star = \arg\min_q \rho_{CV}(q)$ (for any reasonable r).

D. Multibatch SSARX rehash

The simple idea of merging data matrices from different batches for least-squares estimation of VARXs can be recycled for the SSARX SIM [12]. A few logistical considerations are needed however. A superscript $(\cdot)^{(b)}$ indexes batches in the following presentation. Some notation is borrowed from [10].

Assuming a large enough past horizon p such that $A_K^p \approx 0$ the fundamental SIM data equation is

$$\mathbf{y}_f(k) = \bar{H}_{fp}\mathbf{z}_p(k) + \bar{G}_f\mathbf{z}_{f-1}(k) + \bar{D}_f\mathbf{u}_f(k) + \mathbf{e}_f(k) \tag{13}$$

The future horizon signal vectors are

$$\mathbf{z}_{f-1}(k) = \begin{pmatrix} \mathbf{z}(k) \\ \mathbf{z}(k+1) \\ \vdots \\ \mathbf{z}(k+f-2) \end{pmatrix} \tag{14}$$

and

$$\mathbf{y}_f(k) = \begin{pmatrix} \mathbf{y}(k) \\ \mathbf{y}(k+1) \\ \vdots \\ \mathbf{y}(k+f-1) \end{pmatrix} \tag{15}$$

with $\mathbf{u}_f(k)$ and $\mathbf{e}_f(k)$ stacked the same way as (15). Further

$$\bar{G}_f = \begin{pmatrix} 0 & 0 & \dots & 0 \\ H(1) & 0 & \dots & 0 \\ \vdots & \vdots & \ddots & \vdots \\ H(f-1) & H(f-2) & \dots & H(1) \end{pmatrix} \tag{16}$$

$$\bar{H}_{fp} = \begin{pmatrix} H(1) & H(2) & \dots & H(p) \\ H(2) & H(3) & \dots & H(p+1) \\ \vdots & \vdots & \ddots & \vdots \\ H(f) & H(f+1) & \dots & H(f+p-1) \end{pmatrix} \tag{17}$$

and

$$\bar{D}_f = I_f \otimes D \tag{18}$$

where I_f is the identity matrix in $\mathbb{R}^{f\times f}$, $\otimes$ the Kronecker product operator and D the direct feedthrough matrix of the system. The block Markov coefficients $H(j)$ in (16) and (17) can be expressed in terms of the state-space matrices (in case these are known) as $H(j) = CA_K^{j-1}B_K$.

At this stage the multibatch VARX procedure of subsection III-C is invoked to preestimate Markov coefficients to prefill (16) and (18) wich are used for preprocessing of all batches b to form

$$\tilde{\mathbf{y}}_f^{(b)}(k) = \mathbf{y}_f^{(b)}(k) - \bar{G}_f \mathbf{z}_{f-1}^{(b)}(k) - \bar{D}_f \mathbf{u}_f^{(b)}(k) \tag{19}$$

and to construct the data matrices

$$\tilde{Y}_f^{(b)} = \begin{pmatrix} \tilde{\mathbf{y}}_f^{(b)}(k_1) & \dots & \tilde{\mathbf{y}}_f^{(b)}(k_2^{(b)}) \end{pmatrix} \tag{20a}$$

$$Z_p^{(b)} = \begin{pmatrix} \mathbf{z}_p^{(b)}(k_1) & \dots & \mathbf{z}_p^{(b)}(k_2^{(b)}) \end{pmatrix} \tag{20b}$$

whith $k_1 = p+1$ and $k_2^{(b)} = N_b - f + 1$. Matrices (20) are joined into

$$\tilde{Y}_f = \begin{pmatrix} \tilde{Y}_f^{(1)} & \dots & \tilde{Y}_f^{(n_b)} \end{pmatrix} \tag{21a}$$

$$Z_p = \begin{pmatrix} Z_p^{(1)} & \dots & Z_p^{(n_b)} \end{pmatrix} \tag{21b}$$

Matrices (21) are now analysed using canonical correlations [23], [12]:

$$R_{\tilde{\mathbf{y}}_f\tilde{\mathbf{y}}_f} = \tilde{Y}_f \tilde{Y}_f^T \tag{22a}$$

$$R_{\mathbf{z}_p\mathbf{z}_p} = Z_p Z_p^T \tag{22b}$$

$$M = R_{\tilde{\mathbf{y}}_f\tilde{\mathbf{y}}_f}^{-1/2} \tilde{Y}_f Z_p^T R_{\mathbf{z}_p\mathbf{z}_p}^{-1/2} \tag{22c}$$

Calculate the singular value decomposition of M: $M = U\Sigma V^T$ and define the projection matrix

$$J_n = V_n^T R_{\mathbf{z}_p\mathbf{z}_p}^{-1/2} \tag{23}$$

where V_n is the first n columns of V. The state sequence estimate is now $\hat{\mathbf{x}}(k) = J_n \mathbf{z}_p(k)$. The state dimension n may be selected by inspecting the decay of the singular values. Valid dimensions are $1 \le n \le fn_y$.

Matrix (23) is now employed to compose the final multi-batch least-squares equations for the state space matrices. Let $\hat{\mathbf{x}}^{(b)}(k) = J_n \mathbf{z}_p^{(b)}(k)$ and form

$$\hat{X}_n^{(b)} = \begin{pmatrix} \hat{\mathbf{x}}^{(b)}(p+1) & \dots & \hat{\mathbf{x}}^{(b)}(N_b) \\ \mathbf{u}^{(b)}(p+1) & \dots & \mathbf{u}^{(b)}(N_b) \end{pmatrix} \tag{24a}$$

$$Y_n^{(b)} = \begin{pmatrix} \mathbf{y}^{(b)}(p+1) & \dots & \mathbf{y}^{(b)}(N_b) \end{pmatrix} \tag{24b}$$

and

$$\hat{X}_{n,1}^{(b)} = \begin{pmatrix} \hat{\mathbf{x}}^{(b)}(p+2) & \dots & \hat{\mathbf{x}}^{(b)}(N_b) \end{pmatrix} \tag{25a}$$

$$\hat{X}_{n,z}^{(b)} = \begin{pmatrix} \hat{\mathbf{x}}^{(b)}(p+1) & \dots & \hat{\mathbf{x}}^{(b)}(N_b-1) \\ \mathbf{z}^{(b)}(p+1) & \dots & \mathbf{z}^{(b)}(N_b-1) \end{pmatrix} \tag{25b}$$

for $b = 1 \dots n_b$. Join the batches

$$\hat{X}_n = \begin{pmatrix} \hat{X}_n^{(1)} & \dots & \hat{X}_n^{(n_b)} \end{pmatrix} \tag{26a}$$

$$Y_n = \begin{pmatrix} Y_n^{(1)} & \dots & Y_n^{(n_b)} \end{pmatrix} \tag{26b}$$

$$\hat{X}_{n,1} = \begin{pmatrix} \hat{X}_{n,1}^{(1)} & \dots & \hat{X}_{n,1}^{(n_b)} \end{pmatrix} \tag{26c}$$

$$\hat{X}_{n,z} = \begin{pmatrix} \hat{X}_{n,z}^{(1)} & \dots & \hat{X}_{n,z}^{(n_b)} \end{pmatrix} \tag{26d}$$

for estimation of the system $(\hat{A}_K, \hat{B}_K, \hat{C}, \hat{D})$ as follows.

$$\begin{pmatrix} \hat{C} & \hat{D} \end{pmatrix} = Y_n \hat{X}_n^T \left(\hat{X}_n \hat{X}_n^T \right)^{-1} \tag{27}$$

$$\begin{pmatrix} \hat{A}_K & \hat{B}_K \end{pmatrix} = \hat{X}_{n,1} \hat{X}_{n,z}^T \left(\hat{X}_{n,z} \hat{X}_{n,z}^T \right)^{-1} \tag{28}$$

The extraction of $\hat{A}$, $\hat{B}$ and $\hat{K}$ is dictated by the relations (4). Finally, the initial states (for $b = 1 \dots n_b$) can be estimated by forming the observability matrix

$$\hat{O}_f = \begin{pmatrix} \hat{C} \\ \hat{C}\hat{A}_K \\ \vdots \\ \hat{C}\hat{A}_K^{f-1} \end{pmatrix} \tag{29}$$

and matrices (16) and (18), all from the hatted quantities of equations (27) and (28). The data relation [10]

$$\mathbf{y}_f^{(b)}(k) - \hat{\bar{G}}_f \mathbf{z}_{f-1}^{(b)}(k) - \hat{\bar{D}}_f \mathbf{u}_f^{(b)}(k) = \hat{O}_f \hat{\mathbf{x}}^{(b)}(k) + \mathbf{e}_f^{(b)}(k) \tag{30}$$

is then invoked with $f = p$ and $k = 1$ to pose a least-squares problem for $\hat{\mathbf{x}}^{(b)}(1)$. The innovations are obtained by

patching together the residuals generated by (27) and (30). This concludes the multibatch SSARX method[1,2].

E. A delete-batch grouped jackknife

For the particular application it turns out to be convenient to utilise a grouped jackknife procedure [24] for the estimation of the standard errors of the multibatch SIM estimates[3]. The natural mutual exclusive groups of data are the batches themselves. In this subsection a generic scalar estimator $\hat{\theta} = \hat{\theta}(\mathcal{D}_{\mathcal{B}})$ is adopted. $\hat{\theta}$ should be thought of as a function of the output $(\hat{A}, \hat{B}, \hat{C}, \hat{D}, \hat{K})$ of the multibatch SIM introduced above.

The basic delete-m jackknife assumes all groups to be of equal size but this is not quite true for the batches of time-series vector data in the present work. After data pretreatment slicing [11], the batches differ slightly in their respective N_b. Therefore it appears worthwhile to also try the so-called delete-m_j jackknife [24] wich is designed for unevenly sized groups of data.

Let $\mathcal{D}_{\mathcal{B}(j)}$ denote the set of $n_b - 1$ batches formed by removing batch j from the set $\mathcal{D}_{\mathcal{B}}$. SIM application on the set $\mathcal{D}_{\mathcal{B}(j)}$ yields the estimate $\hat{\theta}_{(j)}$, $j = 1 \dots n_b$, whereas SIM application on the full dataset yields the estimate $\hat{\theta}$. Let $\bar{\theta}_{(m)} = (1/n_b)\sum_{j=1}^{n_b} \hat{\theta}_{(j)}$. $m_j = N_j$ denotes the record length of the omitted batch j, $n = \sum_{j=1}^{n_b} m_j$ and $h_j = n/m_j$. Let also $\tilde{\theta}_{(j)} = h_j\hat{\theta} - (h_j - 1)\hat{\theta}_{(j)}$ and $\hat{\theta}_{J(m_j)} = n_b\hat{\theta} - \sum_{j=1}^{n_b}(1 - m_j/n)\hat{\theta}_{(j)}$. The delete-$m$ jackknifed standard error σ_m estimate is defined by

$$\sigma_m^2 = \frac{n_b - 1}{n_b} \sum_{j=1}^{n_b} \left\{ \hat{\theta}_{(j)} - \bar{\theta}_{(m)} \right\}^2 \tag{31}$$

and the delete-m_j ditto σ_{m_j} by

$$\sigma_{m_j}^2 = \frac{1}{n_b} \sum_{j=1}^{n_b} \frac{1}{h_j - 1} \left\{ \tilde{\theta}_{(j)} - \hat{\theta}_{J(m_j)} \right\}^2 \tag{32}$$

Equation (32) reduces to equation (31) in case all m_j are equal. For the present application these expressions are anticipated to be evaluated to approximately the same value.

IV. EXPERIMENTAL DATA ANALYSIS

A vacuum dataset from open-loop operation consisting of $n_b^{\text{vac}} = 40$ batches totaling $N^{\text{vac}} = 34040$ vector samples was acquired from dithering T2R and is here denoted $\mathcal{D}_{\mathcal{B}}^{\text{vac}}$. A plasma dataset $\mathcal{D}_{\mathcal{B}}^{\text{pla}}$ acquired from mandatory closed-loop dithered operation of T2R was also packaged, with $n_b^{\text{pla}} = 74$ and a total $N^{\text{pla}} = 33113$. Detrending was performed to remove possible axisymmetric drifts. Scaling was done such that the signals obtained unity root mean square magnitude. No prefiltering was done.

TABLE I

MAXIMUM EIGENVALUE MAGNITUDE, $\hat{\theta} = \max_j |\lambda_j(\hat{A})|$, AND JACKKNIFED ESTIMATOR STANDARD ERRORS FOR THE T2R PLASMA RESPONSE USING VARIOUS CASCADE SIM RECIPES WITH THE MULTIBATCH SSARX METHOD.

Data	$\hat{\theta}$	σ_m	σ_{m_j}
$\{\tilde{\mathbf{u}}, \mathbf{y}\}$, $D = 0$	1.0292	5.81×10^{-4}	5.90×10^{-4}
$\{\tilde{\mathbf{u}}, \mathbf{y}\}$, $D \neq 0$	1.0291	6.00×10^{-4}	6.07×10^{-4}
$\{\hat{\mathbf{u}}_{\hat{F}}, \mathbf{y}\}$, $D = 0$	1.0292	5.64×10^{-4}	5.66×10^{-4}
$\{\hat{\mathbf{u}}_{\hat{F}}, \mathbf{y}\}$, $D \neq 0$	1.0292	5.88×10^{-4}	5.90×10^{-4}
$\{\hat{\mathbf{y}}_{0\|1}, \mathbf{y}_1\}$, $D \neq 0$	1.0292	4.76×10^{-4}	4.79×10^{-4}
$\{\hat{\mathbf{y}}_{0\|1}, \delta\mathbf{y}\}$, $D = 0$	1.0294	4.61×10^{-4}	4.64×10^{-4}

An initial blocked CV, using a blocksize of $r = 1000$ (to save computational time), suggested the VARX order $q^* \approx 10$ for the input-output data $\{\tilde{\mathbf{u}}, \mathbf{y}\}$. It has been argued that CV may suggest too small lag orders when the objective is accurate identification of the underlying physical processes and not merely signal prediction [26], [27]. This argument, in combination with a shallow minimum of $\rho_{CV}(q)$ (on the large-q side), lead to the selection of $f = p = q = 15$ for the SIM horizons for estimation of G and $f = p = q = 10$ for estimation of F, when applicable. No SVD truncation was done for any of the SIM estimates. All empirical system state dimensions were defaulted to $n = n_y f$.

The maximal eigenvalue modulus of the $\hat{A}$-matrix, using the multibatch SSARX method, for the various cascade SIM recipes above, are presented in Table I. The delete-batch jackknife standard errors are also given. Specifically

$$\hat{\theta} = \max_j \left| \lambda_j \left(\hat{A} \right) \right| \tag{33}$$

where $\lambda_j(\cdot)$ picks out the jth eigenvalue of a matrix. It can be seen that all cascade SIM recipes produce similar results. Note that the standard error estimates pertain to the final dataset given to the SIM and does not include the additional uncertainties induced by filtering or simulation pretreatments.

It turns out that the eigenvector corresponding to the maximally unstable eigenvalue can be mapped directly to the theoretical monochromatic Fourier eigenmode with poloidal mode number 1 and toroidal mode number -11. This can be seen by projection onto the output array using $\hat{C}$. Also in theory is $(1, -11)$ the most unstable. This modal visualisation procedure for state space systems was developed earlier [28], [29] and is reinvoked here to hint at the empirical modal structure of Γ. The result is drawn in Figure 3.

An RFP researcher is likely to recognise the essentials of the typical RFP-theory ideal MHD resistive-shell mode structure in Figure 3. There are admittedly a few question marks for some of the features at the left and right fringes of the plot but a discussion of these is beyond the scope of this work.

[1]It is possible to iterate SSARX by replacing the VARX preestimate with the Markov coefficients implied by the obtained system matrices and then repeat the entire algorithm. When the Markov coefficients cease to change significantly, the iterated SSARX stops. Iterations were not used in this work.

[2]Enforcement of a zero direct feedthrough reduces to a special case of the outlined algorithm; appropriate truncations of the matrices and equations above are done when D should not be present.

[3]Another possibility would be a nonparametric bootstrap resampling [25] of the batches, which can be seen as independent identically distributed random outcomes. That same reasoning also motivates the batchwise jackknife. Bootstrapping may be more accurate but is also expected to be more time-consuming.

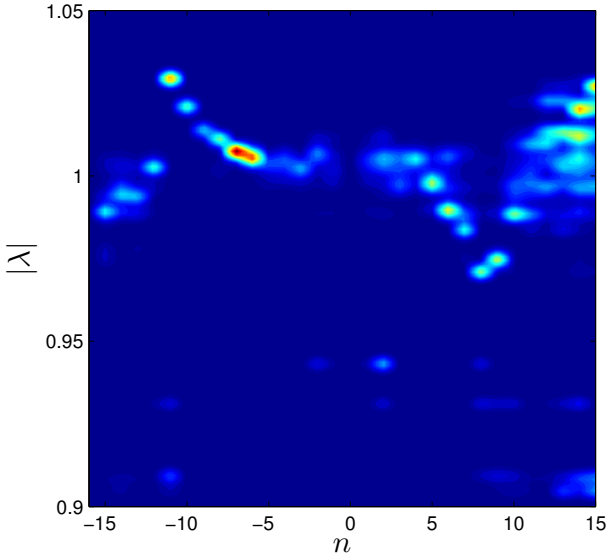

Fig. 3. T2R empirical mode visualisation. $\hat{A}$-matrix eigenvalue magnitude is on the vertical axis and toroidal mode number n is along the horizontal axis. The colouring shows the spatial Fourier power spectrum of the projected (by $\hat{C}$) eigenvectors.

V. CONCLUSIONS

The SSARX subspace system identification method of Janssson [12] was remixed for the purpose of accomodating multibatch data. Two particular cascade structures in the identification problem were explicitly handled by filtering and simulation, respectively. The experimental data from the RFP machine T2R was analysed using these multistep applications of the proposed SIM. The aim of developing the SIM as a scientific measurement technique for MHD modal estimation lead to the formulation of jackknifed standard error estimation based on a natural multibatch data partitioning. It was noted that the multibatch SSARX method appears to pick up empirical plasma response modes that, jointly, indeed resemble the theoretical RFP spectrum. This is encouraging.

ACKNOWLEDGEMENTS

The authors acknowledge support from the EURATOM fusion research programme through the contract of association EURATOM-VR.

REFERENCES

[1] IOP, "Fusion as en energy source - challenges and opportunities," *Institute of Physics Reports*, September 2008. [Online]. Available: http://www.iop.org

[2] R. Hawryluk, D. Campbell, G. Janeschitz, P. Thomas, R. Albanese *et al.*, "Principal physics developments evaluated in the ITER design review," *Nuclear Fusion*, vol. 49, no. 6, p. 065012.

[3] J. Wesson, *Tokamaks*, 3rd ed., ser. International Series of Monographs in Physics. New York: Oxford Science Publications, 2004, no. 118.

[4] "International thermonuclear experimental reactor (ITER) website," February 2010. [Online]. Available: http://www.iter.org

[5] H. Goedbloed and S. Poedts, *Principles of Magnetohydrodynamics*, 1st ed. Cambridge University Press, 2004.

[6] H. Goedbloed, R. Keppens, and S. Poedts, *Advanced Magnetohydrodynamics*, 1st ed. Cambridge University Press, 2010.

[7] M. Walker *et al.*, "Emerging applications in tokamak plasma control: Control solutions for next generation tokamaks," *IEEE Control System Magazine*, vol. 26, pp. 35–63, 2006.

[8] M. S. Chu and M. Okabayashi, "Stabilization of the external kink and the resistive wall mode," *Plasma Physics and Controlled Fusion*, vol. 52, no. 12, p. 123001.

[9] T. Evans *et al.*, "Edge stability and transport control with resonant magnetic perturbations in collisionless tokamak plasmas," *Nature Physics*, vol. 2, pp. 419–423, 2006.

[10] S. J. Qin, "An overview of subspace identification," *Computers and Chemical Engineering*, vol. 30, pp. 1502–1513, 2006.

[11] Y. Zhu, *Multivariable System Identification For Process Control*. Elsevier, 2001.

[12] M. Jansson, "Subspace identification and ARX modeling," in *IFAC Symposium on System Identification*, Aug 2003.

[13] B. Wahlberg, M. Jansson, T. Matsko, and M. Molander, "Experiences from subspace system identification - comments from process industry users and researchers," in *Modeling, Estimation and Control*, ser. Lecture Notes in Control and Information Sciences. Springer Berlin / Heidelberg, 2007, vol. 364, pp. 315–327.

[14] T. Söderström, "Errors-in-variables methods in system identification," *Automatica*, vol. 43, no. 6, pp. 939–958, 2007.

[15] H. Bodin and A. Newton, "Reversed-field-pinch research," *Nuclear fusion*, vol. 20, no. 10, pp. 1255–1324, 1980.

[16] P. R. Brunsell, H. Bergsåker, M. Cecconello, J. R. Drake, R. M. Gravestijn, A. Hedqvist, and J.-A. Malmberg, "Initial results from the rebuilt EXTRAP T2R RFP device," *Plasma Physics and Controlled Fusion*, vol. 43, no. 11, pp. 1457–1470.

[17] P. R. Brunsell *et al.*, "Feedback stabilization of multiple resistive wall modes," *Physical Review Letters*, vol. 93, no. 22, p. 225001, 2004.

[18] E. Olofsson, H. Hjalmarsson, C. R. Rojas, P. Brunsell, and J. R. Drake, "Vector dither experiment design and direct parametric identification of reversed-field pinch normal modes," *Proceedings of the 48th IEEE Conference on Decision and Control CDC/CCC 2009*, pp. 1348 –1353, dec. 2009.

[19] V. D. Pustovitov, "Decoupling in the problem of tokamak plasma response to asymmetric magnetic perturbations," *Plasma Physics and Controlled Fusion*, vol. 50, no. 10, p. 105001.

[20] A. H. Boozer, "Feedback equations for the wall modes of a rotating plasma," *Physics of Plasmas*, vol. 6, no. 8, pp. 3180–3187, 1999.

[21] R. A. Horn and C. R. Johnson, *Matrix Analysis*. Cambridge University Press, 1990.

[22] T. Söderström and P. Stoica, *System identification*. Prentice Hall, 1989.

[23] W. E. Larimore, "System identification, reduced-order filtering and modeling via canonical variate analysis," in *American Control Conference, 1983*, 1983, pp. 445 –451.

[24] F. M. T. A. Busing, E. Meijer, and R. V. D. Leeden, "Delete-m jackknife for unequal m," *Statistics and Computing*, no. 9, pp. 3–8, 1999.

[25] B. Efron and R. J. Tibshirani, *An introduction to the bootstrap*, ser. Monographs on Statistics and Applied Probability. Chapman & Hall / CRC, 1994.

[26] C. Duchesne and J. F. MacGregor, "Jackknife and bootstrap methods in the identification of dynamic models," *Journal of Process Control*, vol. 11, no. 5, pp. 553–564, 2001.

[27] H. V. der Auweraer and B. Peeters, "Discriminating physical poles from mathematical poles in high order systems: use and automation of the stabilization diagram," in *Proceedings of the 21st IEEE Instrumentation and Measurement Technology Conference (IMTC)*, vol. 3, May 2004, pp. 2193 – 2198.

[28] E. Olofsson, C. R. Rojas, H. Hjalmarsson, P. Brunsell, and J. R. Drake, "Closed-loop MIMO ARX estimation of concurrent external plasma response eigenmodes in magnetic confinement fusion," *Proceedings of the 49th IEEE Conference on Decision and Control CDC*, dec. 2010.

[29] K. E. J. Olofsson, P. R. Brunsell, C. R. Rojas, J. R. Drake, and H. Hjalmarsson, "Predictor-based multivariable closed-loop system identification of the EXTRAP T2R reversed field pinch external plasma response," *Plasma Physics and Controlled Fusion*, vol. 53, no. 8, p. 084003, 2011.